Chemistry & Biology
Article

PAP Inhibitor with In Vivo Efficacy Identified by *Candida albicans* Genetic Profiling of Natural Products

Bo Jiang,[1,6] Deming Xu,[1,6] John Allocco,[2] Craig Parish,[3] John Davison,[1] Karynn Veillette,[1] Susan Sillaots,[1] Wenqi Hu,[1] Roberto Rodriguez-Suarez,[1] Steve Trosok,[1] Li Zhang,[1] Yang Li,[1] Fariba Rahkhoodaee,[1] Tara Ransom,[1] Nick Martel,[1] Hao Wang,[1] Daniel Gauvin,[1] Judyann Wiltsie,[2] Douglas Wisniewski,[2] Scott Salowe,[2] Jennifer Nielsen Kahn,[2] Ming-Jo Hsu,[2] Robert Giacobbe,[2] George Abruzzo,[2] Amy Flattery,[2] Charles Gill,[2] Phil Youngman,[2] Ken Wilson,[3] Gerald Bills,[4] Gonzalo Platas,[4] Fernando Pelaez,[4] Maria Teresa Diez,[4] Sarah Kauffman,[5] Jeff Becker,[5] Guy Harris,[3] Paul Liberator,[2] and Terry Roemer[1,*]

[1]Center of Fungal Genetics, Merck Frosst Canada & Co., 225 President Kennedy West, Suite 2550, Montreal, Quebec H2X 3Y8, Canada
[2]Department of Infectious Disease
[3]Department of Medicinal Chemistry
Merck & Co., Inc., 126 East Lincoln Avenue, Rahway, New Jersey 07065, USA
[4]Centro de Investigación Básica (CIBE), Merck Research Laboratories, Merck, Sharp and Dohme de España, S.A. Josefa Valcárcel 38, 28027 Madrid, Spain
[5]Department of Microbiology, University of Tennessee, Knoxville, TN 37996, USA
[6]These authors contributed equally to this work.
*Correspondence: terry_roemer@merck.com
DOI 10.1016/j.chembiol.2008.02.016

SUMMARY

Natural products provide an unparalleled source of chemical scaffolds with diverse biological activities and have profoundly impacted antimicrobial drug discovery. To further explore the full potential of their chemical diversity, we survey natural products for antifungal, target-specific inhibitors by using a chemical-genetic approach adapted to the human fungal pathogen *Candida albicans* and demonstrate that natural-product fermentation extracts can be mechanistically annotated according to heterozygote strain responses. Applying this approach, we report the discovery and characterization of a natural product, parnafungin, which we demonstrate, by both biochemical and genetic means, to inhibit poly(A) polymerase. Parnafungin displays potent and broad spectrum activity against diverse, clinically relevant fungal pathogens and reduces fungal burden in a murine model of disseminated candidiasis. Thus, mechanism-of-action determination of crude fermentation extracts by chemical-genetic profiling brings a powerful strategy to natural-product-based drug discovery.

INTRODUCTION

Bioactive natural products and their derivatives have historically served as a major source of therapeutic agents for treating infectious diseases (Newman et al., 2003). This success exploits the unique characteristics of microbial-produced small molecules, namely, their immense chemical diversity, intrinsic cell permeability, and bioactive specificity, which are typically absent from man-made synthetic libraries. Natural products provide privileged chemical scaffolds selected by evolutionary pressures to interact with a diversity of proteins and other biological targets, and a reservoir that can be co-opted for drug development (Yim et al., 2006). Whereas antibiotic discovery has yielded numerous distinct chemical scaffolds (Clardy et al., 2006), existing antifungal structural classes remain limited despite the medical need for more efficacious antifungal agents (Petrikkos and Skiada, 2007).

To discover new antifungal agents from natural sources, a number of challenges must first be met (Koehn and Carter, 2005). Microbial fermentation extracts are highly complex mixtures, often containing multiple bioactive components. Screening unfractionated extracts in biochemical in vitro assays is complicated by the unknown abundance of any target-specific inhibitor relative to other components in the mixture that can cause nonspecific inhibition. Diverse chromatography procedures are available to fractionate extracts; however, their throughput capacity and application prior to assay screening remain limited. Also at issue is target selection, the extent of its biochemical and genetic validation, and its adaptability to high-throughput screening (HTS). Although all essential genes in *Saccharomyces cerevisiae* have been identified (Winzeler et al., 1999), including many of their orthologs in the human fungal pathogens *Candida albicans* (Roemer et al., 2003) and/or *Aspergillus fumigatus* (Hu et al., 2007), it remains unclear which of their individual gene products are susceptible to chemical inhibition (Payne et al., 2007). Finally, an important consideration is how to rapidly dereplicate known and undesirable compounds from novel chemical entities.

To address these challenges, we and others have turned to chemical-genetic profiling strategies (Baetz et al., 2004; Giaever et al., 1999, 2002, 2004; Lum et al., 2004; Rodriguez-Suarez et al., 2007; Xu et al., 2007). To perform such analyses, strain-specific bar codes were introduced into a collection of defined heterozygote deletion mutants to uniquely identify individual

mutants and facilitate their parallel screening in coculture (Giaever et al., 1999; Shoemaker et al., 1996). When challenged with a nonlethal concentration of a growth-impairing compound, individual strains displaying an altered fitness (either reduced or enhanced) within this population are identified by barcode microarray analysis. Surveying chemically induced growth phenotypes broadly across the genome identifies important aspects of the inhibitory compound's mechanism of action (MOA), including its drug target, import, efflux, and metabolism (Giaever et al., 2004; Rodriguez-Suarez et al., 2007; Parsons et al., 2006). Screening natural-product extracts against the viable yeast haploid deletion set of ~5000 strains, Parsons et al. (2006) recently demonstrated that bioactive compounds predicted to share a common MOA could be identified prior to their purification. Furthermore, these authors also reported that a crude extract from a marine organism produced a chemical-genetic profile very similar to that of the purified compound (Parsons et al., 2006).

Here, we report a new, to our knowledge, natural product hereby named parnafungin (poly(A) RNA fungin) and its identification by *C. albicans*-based chemical-genetic profiling of crude fungal fermentation extracts with intrinsic antifungal activity. Characterization of the parnafungin-containing extract was based on its distinct MOA profile, wherein multiple heterozygous mutants corresponding to subunits of the cleavage and polyadenylation (C/P) complex displayed hypersensitivity to the bioactive entity. Bioassay-guided isolation of parnafungin was achieved by iterative reprofiling of the antifungal fractions and by confirming that the purified material matched the profile of the original extract. Mechanistically, the parnafungin profile most closely matches cordycepin—a known natural-product inhibitor of polyadenylation (Muller et al., 1977). Demonstration of parnafungin's molecular target was achieved by using a *S. cerevisiae* cell-free C/P assay, in which 3′ mRNA polyadenylation was preferentially inhibited versus 3′ mRNA cleavage. Parnafungin also inhibited *S. cerevisiae* and *C. albicans* poly(A) polymerase (PAP) in vitro activity at nM levels. Independently isolated parnafungin-resistant *C. albicans* mutants containing a single F115I amino acid substitution in *PAP1* were also identified and shown to be sufficient to confer parnafungin resistance in either PAP allele. Parnafungin displays potent and broad spectrum activity across multiple fungal pathogens as well as efficacy in a murine model of disseminated candidiasis.

RESULTS

C. albicans Fitness Test Profiling and MOA Determination of Bioactive Compounds in Crude Fermentation Extracts

Recently, we described a *C. albicans* Fitness Test (CaFT) assay using a collection of ~2900 bar-coded heterozygote deletion mutants and its utility to predict the MOA of both known and previously uncharacterized pure compounds, including their cognate target(s), as well as potential resistance mechanisms (Rodriguez-Suarez et al., 2007; Xu et al., 2007). Although incomplete in *C. albicans* genome coverage (~45%), this heterozygote strain set is significantly biased toward genes experimentally demonstrated to be required for normal growth of the pathogen (Hu et al., 2007; Roemer et al., 2003). As such, its composition aids the identification of essential proteins inhibited by target-specific inhibitors, including purified natural products (e.g., cerulenin, *FAS1*; tunicamycin, *ALG7*; and brefeldin A, *SEC7*/*ARF2*) (Roemer et al., 2003).

Expanding on these studies, we first tested whether mechanistically informative CaFT profiles could be obtained by using a defined bioactive mixture containing varying concentrations of two natural products. As shown in Figure S1 (see the Supplemental Data available with this article online), equipotent mixtures of cerulenin combined with tunicamycin, brefeldin A, or fluconazole produced additive CaFT profiles reflecting the expected strain depletions of each growth-inhibitory compound. Mixtures containing an increasing concentration of tunicamycin or brefeldin A relative to that of cerulenin produced mechanism-relevant profiles of both activities, but with significantly greater detection of strain depletions correlating with the major activity (Figure S1). As expected, mixtures more significantly adjusted in the ratio between the two activities produced CaFT profiles reflective of only the major activity (data not shown).

To examine whether mechanistically relevant profiles could be obtained from crude natural-product mixtures, unfractionated extracts prepared from fermentation broths of known producers of cerulenin, brefeldin A, and tunicamycin were profiled by CaFT analysis. As shown in Figures 1A–1C, cerulenin (*FAS1*), brefeldin A (*SEC7*, *ARF2*, and *PDR5*), and tunicamycin (*ALG7* and *IAH1*) crude extract profiles were highly related to their corresponding pure bioactive component. LCMS analysis verified the presence of cerulenin, brefeldin A, and tunicamycin in the respective extracts (data not shown). These data demonstrate that CaFT profiling can identify target-specific inhibitory compounds within fungal and actinomycete fermentation broths, and that MOA annotation of crude extracts could be used to guide their selection for further characterization.

Extract ECC577 Is Predicted to Inhibit 3′ mRNA Processing

We screened a collection of fermentation extracts to identify a subset with intrinsic activity against both *C. albicans* and *A. fumigatus* (C.P. et al., unpublished data) and evaluated their potential MOA by using CaFT profiling. Here, we focus on one such extract, ECC577, derived from a culture broth of *Fusarium larvarum* (MF7022), which inhibited growth of *C. albicans*, *C. glabrata*, *C. krusei*, and *A. fumigatus*, but not bacterial pathogens *Staphylococcus aureus* or *Escherichia coli*. CaFT profiling of ECC577 identified *CLP1*, *PCF11*, *YSH1*, *PTA1*, *CFT2*, *MPE1*, *FIP1*, *ERG27*, and *ORF19.7097* (*C. albicans* genome sequence Assembly 19 designation) heterozygotes to be reproducibly and statistically hypersensitive (z-scores $\geq$ 3.5) over a range of growth-inhibitory concentrations tested (Figures 2A and 2C). Additionally, *CFT1* and *YTH1* heterozygotes displayed significant hypersensitivity to ECC577, albeit under only a single growth-inhibitory concentration. Excluding *ERG27*, all of these hypersensitive strains correspond to genes encoding subunits of the eukaryotic mRNA C/P complex (Figure 2B) (Proudfoot, 2004; Zhao et al., 1999). *ORF19.7097* is homologous to the bovine polyadenylate-binding protein 2 (*PABP2*), which stimulates PAP activity by enhancing its binding affinity for the mRNA substrate (Kerwitz et al., 2003). In addition, multiple heterozygote strains corresponding to RNA polymerase II (RNAPII) activity (including *RPO26*, *RPB7*, and *RPB8*) and ribosomal biogenesis (*NOC3*, *NUG1*, *NOP14*, and *UTP22*) reproducibly displayed an apparent resistant phenotype

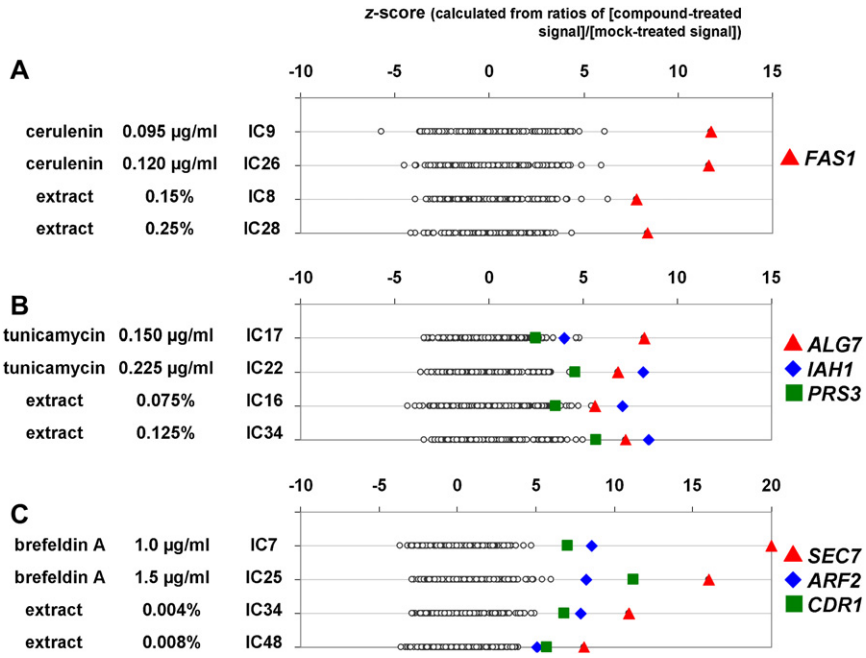

Figure 1. CaFT Profiling of Natural-Product Crude Extracts

(A–C) CaFT profiles of purified (A) cerulenin, (B) tunicamycin, and (C) brefeldin A versus crude extracts of fermentation broths containing the corresponding natural-product activity. Growth-inhibitory concentrations are indicated. The z-scores are displayed one-dimensionally regardless of heterozygous strain identities. Color symbols designate heterozygote strains whose hypersensitivities correspond to the MOA of the tested compounds (see Xu et al., 2007 for details).

in the presence of ECC577. Collectively, these results suggest that the bioactive component present in extract ECC577 may inhibit growth by interfering with mRNA C/P functions.

The CaFT Profile of Cordycepin, a Known Inhibitor of Poly(A) Polymerase Activity

To further characterize ECC577, we first compared its profile to the CaFT profile of a known 3′ mRNA processing inhibitor, cordycepin (3′-deoxyadenosine), which is a toxic adenosine analog produced by *Cordyceps militaris*. Cordycepin is a pro-drug: upon entering cells, it is converted to 3′-dATP, which acts as both an RNA molecule chain terminator and a substrate competitive inhibitor of the PAP (Muller et al., 1977). CaFT profiles of cordycepin were found to be highly related to those of extract ECC577, with multiple components of the mRNA C/P complex (*CLP1*, *PCF11*, *YSH1*, *PTA1*, *CFT1*) similarly displaying heterozygote sensitivity in at least two of the drug concentrations tested (Figures 2A and 2C). Additional strain depletions included *DAL5* and *FOL2*. *PAP1*, which encodes PAP, was conspicuously absent from either ECC577 or cordycepin CaFT profiles. As this could reflect technical issues regarding *PAP1* bar codes (see Discussion), we tested whether *PAP1* heterozygotes and/or other subunits of the C/P complex are hypersensitive to ECC577 and/or cordycepin. Individual heterozygotes comprising the above-described CaFT profiles (including *PAP1*) were directly evaluated by spot tests and were confirmed to be hypersensitive to ECC577 and cordycepin (Figure 2D).

Noteworthy are two heterozygote strains (*ADO1* and *NNT1*) that exhibit significant resistance to cordycepin and are unique to its CaFT profile. *ADO1* (adenosine kinase) is required to convert cordycepin to 3′-dAMP in vivo, and the *ado1* null mutant of *S. cerevisiae* is resistant to cordycepin (Lecoq et al., 2001). *NNT1* codes for a Na^+-independent, H^+-coupled nucleoside symporter (absent in *S. cerevisiae*) with broad nucleoside substrate specificity (Rodriguez-Suarez et al., 2007; Xu et al., 2007), including cordycepin (Loewen et al., 2003). Presumably, heterozygote levels of *C. albicans NNT1* and *ADO1* reduce cordycepin uptake and its conversion to 3′-dATP, respectively, thereby partially alleviating its growth-inhibitory effects.

Interestingly, heterozygotes corresponding to RNAPII that were hyposensitive to ECC577 were not detected in cordycepin CaFT profiles. These differences predict that the MOA of ECC577 and cordycepin, while related, are not identical. Importantly, these data also predict that the bioactive component within ECC577 is structurally distinct from cordycepin, since only cordycepin requires a nucleoside permease for uptake. Indeed, LCMS analyses of the ECC577 extract did not identify cordycepin or other potential nucleoside analogs (data not shown).

Isolation and Structure Elucidation of Parnafungin

To identify the active component in ECC577, a large-scale fermentation of MF7022 was performed, and an acetone extract of this material was used to confirm its original bioactivity by using CaFT profiling (Figures 2A and 2C). Bioactivity-guided purification and structure elucidation were performed by X-ray crystallography and NMR analysis (C.P. et al., unpublished data), revealing a mixture of diastereomers (Figure 2E). CaFT profiling of this purified diastereomer mixture reproduced the CaFT profile of the crude extract (Figures 2A and 2C). Based on its predicted MOA from chemical-genetic profiling, we have named this compound class parnafungin (poly(A) RNA fungin).

The structural novelty of parnafungin resides in the presence of an isoxazolidinone ring not previously reported, to our knowledge, in natural products. It is fused to a xanthone ring system commonly found in natural products, most notably in secalonic acids. Although secalonic acids display broad antimicrobial activity (Reddy and Reddy, 1991) and are potent inhibitors of *C. albicans*, its CaFT profile is unrelated to parnafungin (Table S1). Moreover, a derivative of parnafungin, in which the isoxazolidinone ring was opened due to degradation, does not inhibit the growth of *Candida sp.* (data not shown). Thus, the combined structural features of parnafungin are required for its antifungal activity and selectivity.

Biochemical Characterization of Parnafungin: A Potent Inhibitor of 3′ mRNA Polyadenylation

Consistent with its predicted MOA, parnafungin-treated *C. albicans* cells show depleted poly(A)$^+$ RNA transcript levels

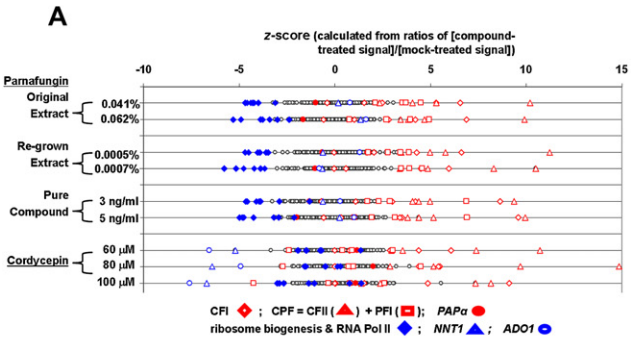

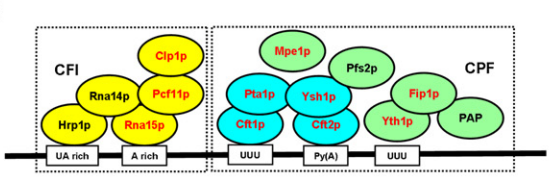

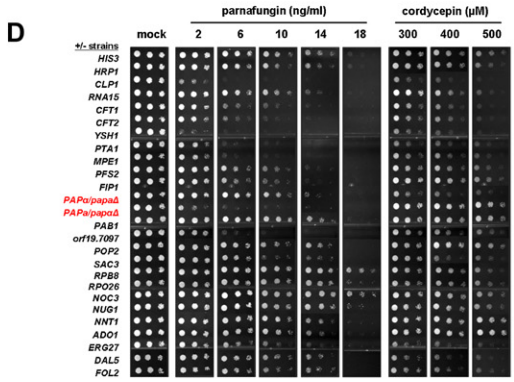

C

parnafungin origial extract %		parnafungin regrown extract %		parnafungin compound ng/ml		cordycepin µM			orf19	gene	relevance to MOA
0.041 (IC59)	0.062 (ID65)	0.0005 (IC37)	0.0007 (IC53)	3.0 (IC51)	5.0 (IC64)	60 (IC35)	80 (IC59)	100 (IC64)			
6.562	6.8711	6.6183	5.9634	8.6408	9.5871	6.0515	5.4773	9.1228	6931	CLP1	Cleavage Factor I = CFI (Zhao et al., 1999)
5.2922	4.186	1.6715	4.4939	4.2022	3.5194	4.3717	4.3721	4.8491	684	PCF11	
2.4955	2.8229	4.2626	3.4572	2.9766	3.4003	2.8773	5.408	1.5188	4538	RNA15	
-0.395	-0.5834	-0.0388	-0.0579	-0.7175	-0.5753	0.7704	0.8244	0.0321	1531	RNA14	
1.5376	1.0286	2.0485	0.5824	1.082	0.3109	0.0022	0.0023	0.0019	5989	HRP1	
10.2069	9.9166	11.2125	10.4892	9.3639	9.9446	10.7356	14.8594	7.3612	5486	YSH1	Cleavage Factor II = CFII (Zhao et al., 1999)
5.2976	4.6685	5.7762	8.3031	4.9792	5.1523	7.3759	9.707	8.1381	7041	PTA1	
4.0598	3.449	4.9655	4.8684	4.3822	3.789	2.9602	2.8951	1.3893	325	CFT2	
2.3513	3.85	3.4575	3.4019	4.0689	4.3846	3.5613	5.1452	2.362	2760	CFT1	
4.5111	3.9405	3.8641	4.5705	6.8642	6.9289	3.0401	4.4924	2.5907	4628	MPE1	Polyadenylation Factor I = PFI (Zhao et al., 1999)
3.5607	2.707	2.7719	3.8963	2.8788	3.1346	0.4012	0.7159	-0.333	6881	YTH1	
3.7415	4.9197	3.4471	3.47	2.2865	1.9481	-2.401	-2.7338	-4.2489	4258	FIP1	
2.1303	0.7572	1.7486	3.4733	1.7258	0.9995	0.8927	0.9699	0.8143	2307	PFS2	
-0.9971	-1.6668	-0.6781	-1.0166	-1.3335	-1.9742	1.1473	2.0165	1.0831	3197	PAPα	poly(A) polymerase
3.7058	4.086	4.3479	5.6552	4.252	4.8721	3.5892	1.8875	1.9608	7097	PABP2	poly(A) binding
2.4007	2.5581	2.6505	4.1187	3.7062	4.7653	1.844	0.8014	1.2673	5771	PBP2	
-1.2478	-1.1613	-0.4447	-1.3682	-1.0079	-0.7419	-1.9131	-2.8331	-2.9521	3037	PAB1	
-0.8183	-0.7741	-1.1781	-0.513	-2.6113	-0.8135	0.0022	0.0976	0.0019	3333	NAB2	
-1.1917	0.735	0.4507	-0.555	0.3363	0.1293	-1.0361	-1.729	0.0281	4764	PAN2	poly(A) shortening
-0.6419	-1.7922	0.3081	-1.4089	-0.5277	-1.1584	0.5921	0.1574	-0.6357	4010	PAN3	
-3.8486	-3.5874	-3.5477	-4.0705	-2.3121	-2.7672	-3.9629	-2.529	-1.8221	5734	POP2	mRNA deadenylase
0.9189	0.4673	0.8878	1.9137	0.6638	0.1907	2.413	3.8459	3.0506	1555	SAC3	polyA+ RNA transport
-3.1201	-3.7757	-3.9163	-4.2062	-3.8912	-4.2528	-0.7103	0.2799	-1.367	7197	NOC3	ribosome biogenesis
-4.0078	-2.9909	-4.7097	-5.8025	-2.9136	-2.9324	-1.4951	-1.5959	-1.0567	2917	NUG1	
-4.2958	-3.4246	-3.4669	-3.8844	-4.1129	-3.1781	-0.7605	0.1262	1.3711	5959	NOP14	
-4.6876	-2.3729	-3.5995	-4.7633	-1.3081	-2.1461	1.3449	-0.532	0.7537	1569	UTP22	
-4.2144	-3.8998	-3.6026	-3.8898	-4.6724	-4.7727	-1.4727	-1.5061	-3.0228	6314	RPB8	RNA pol II
-4.3859	-5.3095	-4.5062	-3.6587	-3.964	-4.8483	-1.9375	-0.4982	-2.8846	2643	RPO26	
-4.5999	-4.916	-4.046	-5.1644	-4.5936	-4.9792	-1.9035	-1.5305	-2.6808	3347	RPB7	
0.1897	1.3405	-0.6366	-0.679	-0.6408	0.2513	-5.1948	-6.4307	-6.7101	4118	NNT1	uptake (CDC)
0.8105	1.6569	1.3225	-0.8064	0.2724	1.0314	-6.5423	-4.9173	-7.582	5591	ADO1	activation (CDC)
4.4941	6.2208	2.8824	2.5973	1.5868	2.4378	4.4894	3.3501	2.8815	3240	ERG27	unknown
2.0879	3.1975	2.8407	1.2399	4.3936	5.2609	0.0011	0.0012	0.0009	7293	MPS1	
2.1653	2.211	2.644	0.9951	3.0748	3.3008	0.0022	-4.7602	-4.614	1791	MAK11	
-1.4364	-1.6445	-0.7311	-2.2014	0.0211	-1.252	4.5042	4.5486	5.5444	309	DAL5	
0.5576	0.4262	0.5812	0.6212	0.7443	1.2485	2.0239	4.4704	7.3533	3957	FOL2	
0.808	-0.2628	0.4389	0.6043	0.6595	0.0082	-2.5841	-2.8672	-4.1205	5610	ARG3	
-3.5385	-3.0929	-3.6009	-3.0997	-4.2298	-4.5381	-0.7879	-0.3571	-0.9651	1214	MAP2	

(z ≥ 3.5000)
(2.000 ≤ z < 3.5000)
(-2.0000 < z < 2.000)
(-3.500 < z ≤ -2.0000)
(z ≤ -3.5000)

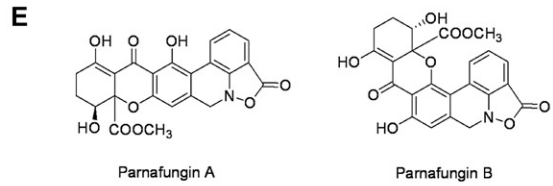

Figure 2. CaFT Profiling of Parnafungin-Containing Extracts versus Cordycepin and Parnafungin Pure Compounds

(A) CaFT profiles of the *Fusarium larvarum* original crude extract (ECC577), its regrowth extract, purified parnafungin, and cordycepin. Six representative CaFT experiments of parnafungin (two each for the original and regrowth extracts and purified compound) and three of cordycepin were combined for comparison. The z-scores are displayed one-dimensionally regardless of heterozygous strain identities. Color symbols designate heterozygote strains whose hypersensitivities correspond to the MOA of the tested compounds. CFI, cleavage factor I; CPF, cleavage and polyadenylation factor; CFII, cleavage factor II; PFI, polyadenylation factor I.

(B) A schematic representation of the yeast C/P complex (adapted from Zhao et al., 1999, also see the reference for *cis*-acting elements in the precursor RNA). Highlighted in red are the genes whose corresponding heterozygous strains are hypersensitive to parnafungin. CFII subunits are shown in light blue, and PFI subunits are shown in green.

(C) Table representation of the CaFT profiles shown in (A). The most significant responsive heterozygous strains were selected based on the average of their z-scores (≥ 3.000 for hypersensitivity or ≤ -3.000 for resistance) in either of the two sets of experiments. The corresponding genes are grouped according to their cellular functions and the possible relevance to the MOA of parnafungin and cordycepin. Also included (with orf19 designations and genes highlighted in gray) are z-scores of strains that correspond to additional proteins involved in the 3′-end processing but displaying no significant responses in the CaFT experiments.

(D) Validation of the CaFT results by spot tests. Based on the CaFT results shown in (A), representative heterozygous deletion strains were selected (from each group) and tested against parnafungin and cordycepin at multiple concentrations on the YNBD agar media (supplemented with CSM, 2-day growth at 30°C). Also included is the control *HIS3* strain, which is the cogenic parent of all heterozygous strains used in this study. Note that the two alleles of *PAP* genes (red) are named according to their chromosomal location adjacent to the mating-type-like loci. Although a *PAPα/papaΔ* strain is present in the CAFT pool, a *PAPa/papαΔ* strain is not.

(E) Structures of parnafungin A and B.

(Figure S2). Since parnafungin is also active against *S. cerevisiae* (see below), we employed an in vitro C/P assay with a yeast extract as previously described (Chen and Moore, 1992). Incubation of a ^{33}P-labeled precursor RNA substrate with the yeast extract resulted in proper C/P (Figure 3B, lane 2), the latter of which was efficiently blocked in the presence of 3′-dATP (Figure 3B, lane 3). The incorporation of 3′-dATP (cordycepin triphosphate) terminates polyadenylation due to the lack of a 3′-OH group (Muller et al., 1977). Parnafungin inhibited the accumulation of polyadenylated RNA product in a concentration-dependent manner, with concomitant accumulation of the cleaved intermediate (Figure 3B, lanes 5–8). In the presence of 3′-dATP, the cleavage of precursor RNA was not significantly impaired by parnafungin (Figure 3B, lanes 9 and 10).

In an in vitro PAP assay that employed recombinant *S. cerevisiae* Pap1p and tRNA (Lingner et al., 1991), parnafungin was a potent inhibitor with an IC_{50} of 66 ng/ml (145 nM) (Figure 3C). In the PAP assays using a poly(A) substrate, parnafungin inhibited native *C. albicans* PAP activity and the recombinant Papα enzyme with IC_{50} values of 14 and 10 ng/ml (31 and 22 nM), respectively. However, parnafungin also inhibited the recombinant human PAP enzyme at an IC_{50} of 52 ng/ml (114 nM). Thus, chemical modification of parnafungin would be required to achieve further target selectivity. Nonetheless, it was not a general inhibitor of nucleotide polymerase, as the IC_{50} against three human DNA polymerase isoforms was > 50 μM (data not shown). Furthermore, parnafungin is not an ATP-competitive inhibitor of PAP activity (Figure 3D).

Isolation and Characterization of *C. albicans* PAP Mutations that Confer Parnafungin Resistance

To corroborate the inhibitory activity of parnafungin on the PAP enzymes, we performed chemical mutagenesis directly in *C. albicans* to isolate PAP mutations that confer resistance to the inhibitor. As the PAP gene is physically located in the *MAT*-like loci of the genome, and its two alleles encode isoforms sharing ~70% amino acid identity (Hull and Johnson, 1999), a heterozygous deletion strain of *PAPα/papaΔ* and a control *HIS3/his3Δ* strain were first used to generate parnafungin-resistant mutants. After two rounds of selections, 80 and 8 resistant mutants were obtained from these 2 strains, respectively. They were counterscreened for resistance to fluconazole and aureobasidin A (data not shown). Only seven mutants isolated from the *PAPα/papaΔ* strain were resistant specifically to parnafungin. From these mutants, the entire *PAPα* ORFs were PCR amplified and cloned. DNA sequence analyses revealed that strains CA62, CA72, and CA75 contain a single nucleotide alteration in the *PAPα* gene. This T-to-A mutation resulted in an amino acid substitution from Phe to Ile in residue 115 located in the conserved nucleotidyl-transferase domain of PAP proteins (Figure 4A). No mutation in *PAPα* was found in 16 additional crossresistant mutants in the background of the *PAPα/papaΔ* strain (data not shown).

As the surviving cells after the mutagenesis were plated directly on parnafungin-containing media, *papα(F115I)* mutations arose independently. To determine if it is sufficient to confer resistance to parnafungin, we introduced *papα(F115I)* into the parental *PAPα/papaΔ* strain by two-step gene replacement (Figure S3A). After integration of a functional *papα(F115I)* gene (marked by *URA3*) at the *PAPα* locus, the resulting strain (CA153, with two tandem *PAP* genes flanking *URA3*, *PAPα::URA3::papα(F115I)*), showed intermediate resistance to parnafungin (Figure 4B), suggesting that the mutation is semidominant. After counterselection on 5-FOA, a single *PAP* allele was retained. We confirmed that all of the parnafungin-resistant isolates examined contained *papα(F115I)*, whereas the sensitive ones were wild-type (Figure 4B; Figure S3B). By the same method, we introduced the corresponding mutation in *PAPa* in a *PAPa/pap$\alpha\Delta$* strain, and we determined that *papa(F115I)* also confers resistance to parnafungin, is semidominant, and likewise shows no crossresistance to other antifungals tested (Figure 4B and data not shown). These results established that the F115I change in either *C. albicans* PAP isoform is sufficient to alter susceptibility to parnafungin. No significant resistance to cordycepin was observed among assayable *papa(F115I)* or *papα(F115I)* mutants (Figure 4C). We conclude that the F115I substitution specifically confers parnafungin resistance to both PAP isoforms.

In Vitro Microbiological Activity of Parnafungin

Parnafungin whole-cell potency was assessed against a panel of clinically relevant fungal and bacterial pathogens (Table 1). Parnafungin is markedly potent against *C. albicans*, and it displays a minimal inhibitory concentration (MIC) of 14 ng/ml and equivalent potency against clinical and laboratory isolates of *C. albicans* with reduced susceptibility to caspofungin (e.g., CLY1996) (Park et al., 2005). While parnafungin is less potent against two fluconazole-resistant *C. albicans* clinical isolates (Safdar et al., 2001), MICs remain below 1 μg/ml. Parnafungin activity against five additional *Candida sp.* ranged between MIC values of 0.014 and 3.33 μg/ml. Although *A. fumigatus* is less susceptible to parnafungin (MIC = 8–16 μg/ml) (Figure 5A), *A. fumigatus PAP1* and *CFT2* conditional mutants (see below) displayed marked hypersensitivity to parnafungin under partially repressing conditions without altered susceptibility to itraconazole (Figure 5B). Consistent with a eukaryotic-specific MOA, parnafungin did not inhibit the growth of either *S. aureus* or *E. coli* at the highest concentration tested (Table 1).

Multiple Components of the Fungal Cleavage and Polyadenylation Complex Are Essential for Growth of *C. albicans* and *A. fumigatus*

PAP1 and each of 14 core subunits of the C/P complex are essential for *S. cerevisiae* viability (Zhao et al., 1999). To test whether their essentiality is conserved in fungal pathogens, we constructed conditional mutants for 13 predicted orthologs in *C. albicans* and *A. fumigatus* by using tetracycline (Tet)- and nitrate (*NiiA*)-regulatable promoter replacement strategies previously described (Hu et al., 2007; Roemer et al., 2003). An examination of their terminal phenotype under repressing conditions reveals that *PAP* and all 12 subunits tested are essential for *C. albicans* viability (Figure S4). *A. fumigatus PAP1* as well as 10 of 12 predicted C/P orthologs (Table S2) were also experimentally confirmed to be essential (Figure S5). As the Tet- and *NiiA*-regulatable promoters are also effectively repressed in vivo, we tested the consequences of PAP shut-off in a mouse model of candidiasis and aspergillosis, and we demonstrated both pathogens to be avirulent upon genetic inactivation of *PAP1* in vivo (Figures 6A and 6B).

Efficacy of Parnafungin in a Murine Model of Disseminated Candidiasis

Parnafungin's potency against *C. albicans*, even in the presence of 50% mouse serum (MIC = 1.111 μg/ml) (Table 1), as well as the requirement for *PAP1* to support cell growth and virulence in an animal host suggest that parnafungin could display efficacy in an animal model of infection. To evaluate its efficacy, *C. albicans*-infected mice were treated at varying parnafungin doses twice daily for 2 d in an abbreviated candidiasis model (Bartizal et al., 1992), and on the day after the final compound treatment, fungal burden was quantified within kidneys. The observed fungal burden in sham-treated animals reached > 6.3 $\log_{10}$ CFU/g

A

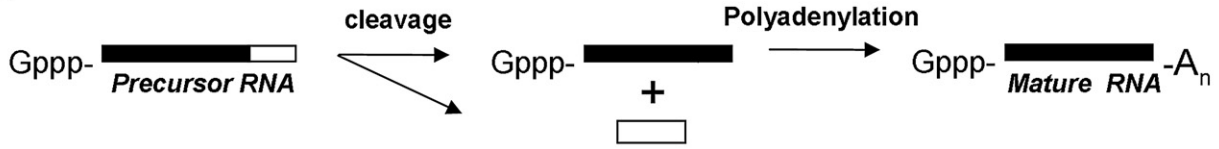

B

CP extract	-	+	+	+	+	+	+	+	+	+
ATP (1 mM)	+	+	-	+	+	+	+	+	-	-
3'-dATP (1 mM)	-	-	+	-	-	-	-	-	+	+
EDTA (1 mM)	-	-	-	+	-	-	-	-	-	-
Parnafungin (μg/mL)	-	-	-	-	120	24	4.8	0.96	68	34

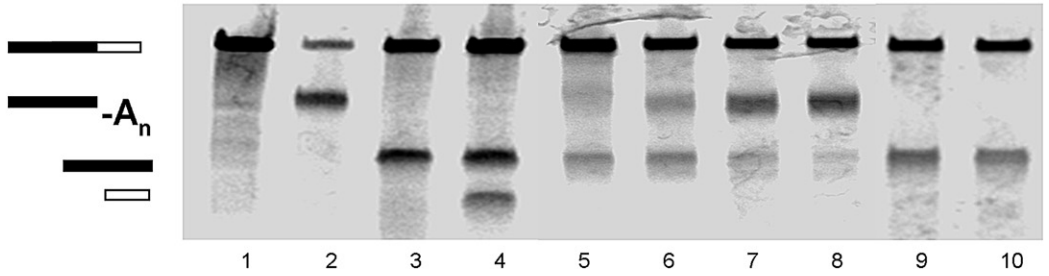

C

Source of PAP enzyme	Substrate RNA	Parnafungin IC_{50} (ng/ml)
S. cerevisiae rPAP1	tRNA	66
C. albicans nPAP	poly(A)	14
C. albicans rPAPα	poly(A)	10
Human rPAP	poly(A)	52

D

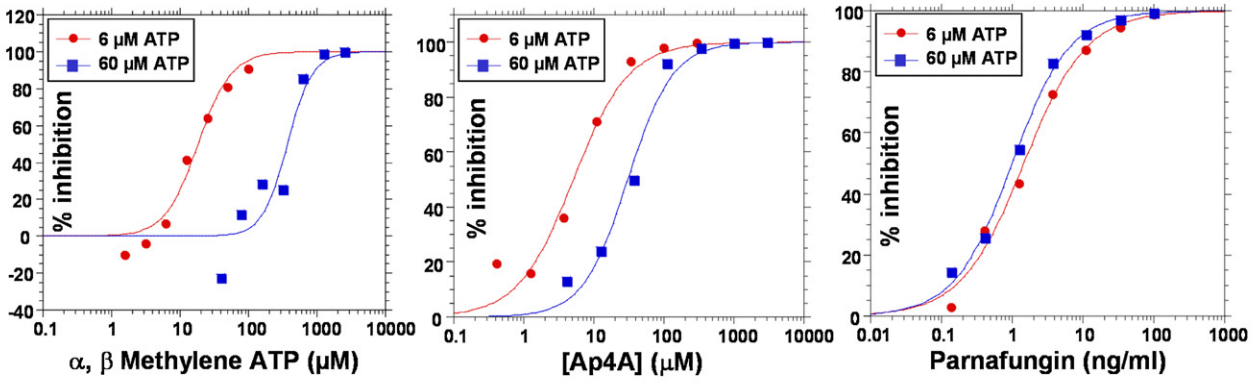

	S. cerevisiae PAP IC_{50}		
ATP (μM)	α,β-methylene ATP	Ap4A	Parnafungin
6	18 μM	5 μM	3.3 nM
60	370 μM	30 μM	2.2 nM

Figure 3. MOA Characterization of Parnafungin
(A) Schematic representation of 3′ mRNA processing.

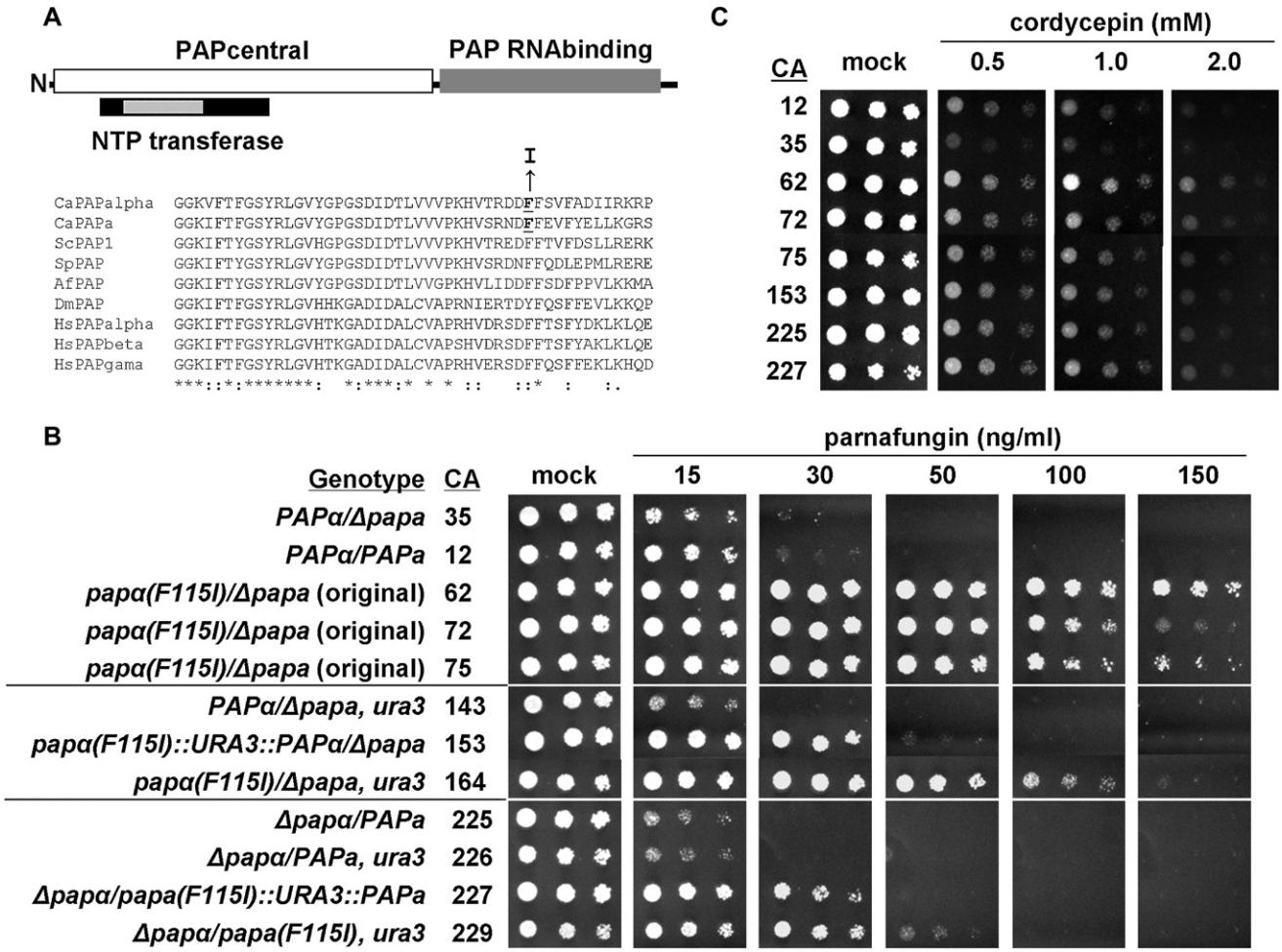

Figure 4. Isolation and Characterization of *C. albicans PAPa* and *PAPα* Mutations Conferring Parnafungin Resistance

(A) The domain structure of PAP (top) and the alignment of the amino acid sequence of a portion (indicated by the hatched bar) of the NTP transferase domain of PAPs (bottom) from *C. albicans* (GenBank accession numbers are provided in the Supplemental Experimental Procedures). The parnafungin-resistant mutations in *Papαp* and *Papap* are indicated.

(B) Susceptibility of relevant strains to parnafungin (on YNBD agar media, supplemented with 2.5 mM uridine), including: a control strain (CA12), the parental heterozygous deletion strain (CA35) used in EMS mutagenesis, and three independent original resistant isolates (CA62, 72, 75) containing the *papα(F115I)* mutation. The starting strains used in the two-step gene replacement are CA413 and CA226, derived from CA35 and CA225, respectively. The pop-in (CA153, 227) and pop-out (CA164, 229) strains are indicated by their genotypes.

(C) Susceptibility of *papa(F115I)*- and *papα(F115I)*-containing mutants to cordycepin. Reconstructed mutant strains are *ura3*$^-$ and require uridine, which, as a competitive substrate for the transporter Nnt1p, suppresses cordycepin (data not shown). Thus, they were not examined for cordycepin susceptibility. Instead, the *URA3* prototrophs (CA62, 72 and 75) and the two pop-in strains (CA153 and 227) were tested. Shown is the 2-day growth on YNBD agar media at 30°C.

kidney. In two independent experiments, animals treated with parnafungin displayed a significant and dose-dependent decrease in fungal burden (Figure 6C). At a dose of 50 mg/kg, the fungal burden decreased by 2.30 and 2.88 $\log_{10}$ CFU/g kidney. The dose capable of reducing *C. albicans* burden by >99% (ED_{99}) was 30.98 and 20.82 mpk, respectively, and no adverse

(B) In vitro assay of C/P using the whole-cell extract (WCE) prepared from *S. cerevisiae*. The ^{33}P-labeled precursor RNA (lane 1) was incubated with the WCE under various conditions for the production of poly(A)$^+$ product (lane 2), the 5′ portion of the intermediates (lane 3, with the polyadenylation reaction blocked by 3′-deoxyl-ATP), and both 5′- and 3′-intermediates (lane 4). Parnafungin, at the concentrations indicated, was added to the reaction under the standard conditions (lanes 5–8), or in the presence of 3′-deoxyl-ATP (lanes 9 and 10). Note that under the standard conditions poly(A)$^+$ product was diminished, and that there was simultaneous accumulation of the 5′-intermediate with increasing concentrations of parnafungin (lanes 5–8), suggesting a preferential inhibition of polyadenylation. Moreover, in the presence of 3′-deoxyl-ATP, which blocks polyadenylation (lanes 3), the accumulation of the 5′-intermediate was also diminished, suggesting a partial inhibition of the cleavage by parnafungin.

(C) Inhibitory effects of parnafungin on polyadenylation of tRNA and poly(A) RNA substrates catalyzed by the indicated PAP enzymes from *S. cerevisiae*, *C. albicans*, and human sources.

(D) Titration of competitive inhibitors of PAP (α, β methylene ATP, Ap4A) and parnafungin against ATP (at 6 and 60 μM) in an in vitro polyadenylation assay with recombinant *S. cerevisiae* Pap1p and poly(A) RNA.

Table 1. The Whole-Cell Inhibitory Activity of Parnafungin

Species	Strain	MIC (μg/ml)[a]
C. albicans	MY1055	0.014
C. albicans (50% mouse serum)	MY1055	1.111
C. albicans	CLY16996[b]	0.014
C. albicans	CLY16998[c]	0.014
C. albicans	JMB4[d]	0.041
C. albicans	395-98[e]	0.123
C. glabrata	ATCC90030	1.111
C. parapsilosis	ATCC220129	1.111
C. lusitaniae	ATCC34449	1.111
C. krusei	ATCC6258	0.014
C. tropicalis	ATCC750	3.333
S. cerevisiae	ATCC201389	3.333
S. aureus	MB2865	>32
E. coli	ATCC25922	>32

[a] MIC was determined in Sabarose Dextrose medium.
[b] The clinical isolate that contains a mutation in *fks1* and is resistant to Candidas (Bartizal et al., 1992).
[c] The clinical isolate from the same patient with a wild-type *FKS1*.
[d] Clinical isolate with fluconazole resistance due to overexpression of *MDR1* (D. Perlin, personal communication).
[e] Clinical isolate with fluconazole resistance due to overexpression of *CDR1*, *CDR2*, and *MDR1* (D. Perlin, personal communication).

effects were observed in any of the parnafungin treatment groups. As the genetic inactivation of PAP under all candidiasis experimental conditions tested (Figure 6A) resulted in a fungal burden often below or near the limit of detection (Table S3), chemical optimization of parnafungin may significantly improve its efficacy. ED_{99} values for the FDA-approved antifungal agents caspofungin and fluconazole were 0.033–0.038 mpk and 0.933–1.004 mpk, respectively.

DISCUSSION

We screened a defined set of *C. albicans* heterozygote deletion mutants largely representing genes required for viability and/or normal growth for their altered sensitivity to growth-inhibitory compounds to identify small molecules that act by a target-specific mechanism. The discovery of parnafungin demonstrates that crude fermentation extracts are assayable and that mechanistically informative chemical-genetic profiles are derived from naturally produced bioactive compounds within complex mixtures. Parnafungin's MOA was verified by both biochemical and genetic means, and its further characterization supports its potential as a new antifungal agent with a unique MOA.

Mechanism-of-Action Profiling of Crude Extracts

Despite the intrinsic challenges of evaluating natural-product extracts, CaFT profiling and upfront MOA annotation of crude extracts may provide a powerful approach to screening and selecting appropriate samples for chemical isolation. Thus, by screening a breadth of potential drug targets, diverse MOAs may be revealed among distinct extracts, and those predicted to affect preferred cellular processes/targets may be prioritized accordingly. Here, we focused on an extract predicted to affect 3′ mRNA maturation, as this process is broadly conserved in eukaryotes and is essential for cell growth among pathogenic fungi (Table S2). As such, the bioactive component is predicted to display broad antifungal activity. Similarly, new or known natural products affecting clinically validated antifungal targets, including cell wall and ergosterol biosynthesis, may be identified and prioritized for follow-up evaluation (unpublished data). Importantly, as bioactive natural products often generally disrupt cell membranes (e.g., polyenes, ionophores), alkylate DNA synthesis (e.g., rachelmycin/CC1065), or impair RNA synthesis (actinomycins), rather than inhibit specific protein targets, such extracts could be avoided. A compendium of chemical-genetic profiles has been used to predict MOA of previously characterized compounds among others that display related profiles (Hughes et al., 2000; Parsons et al., 2006). Here, we demonstrate that new chemical matter with mechanistically defined activity can be discovered. By using even a small reference set of mechanistically significant natural-product profiles, the relatedness of CaFT profiles produced from an undefined crude extract can be compared to the reference set to predict its bioactivity.

Biology

Interestingly, the *C. albicans* PAP gene encodes isoforms sharing only ~70% amino acid identity (Hull and Johnson, 1999). Despite such extreme polymorphisms, we demonstrate that both alleles, *PAPa/papαΔ* and *PAPα/papaΔ*, are functional as heterozygote deletion mutants, display normal growth rates, and are collectively essential, as the Tet-*PAPα/papaΔ* conditional mutant is not viable under Tet-repressing conditions (Figure S4). Parnafungin likely inhibits both PAP isoforms, as both *PAPa/papαΔ* and *PAPα/papaΔ* heterozygotes are hypersensitive to drug treatment (with the *PAPα/papaΔ* heterozygote particularly hypersensitive), and F115I mutations in either PAP allele confer resistance (Figure 4). Surprisingly, CaFT profiles did not identify the *PAP* heterozygote as sensitive to either the parnafungin-containing extract or the pure compound. This is due to suboptimal *PAP* barcodes, which provide low hybridization levels and large standard deviations between experiments (data not shown). Indeed, the predicted MOA for parnafungin (and cordycepin) was not based on the identification of *PAP* within the CaFT profile, but rather on the chemical sensitivity of a functional network of genes encoding subunits of the C/P complex and 3′mRNA processing (Figure 2). We speculate that the biological richness of these profiles reflects synthetic lethal interactions between chemical inhibition of *PAP* and the heterozygosity of other essential subunits of the C/P complex. Parnafungin may also indirectly affect assembly, stability, and/or function of the C/P complex through its inhibition of PAP, as weak effects on 3′ mRNA cleavage were also observed in the cell-free C/P assay despite biochemical and genetic evidence supporting the idea that PAP-mediated polyadenylation is its primary target.

Chemical-genetic profiles of parnafungin and cordycepin also emphasize the important interrelationships between mRNA transcription, its 3′ processing, and degradation. For example, mRNA C/P processing is coupled to its transcription via the C-terminal domain (CTD) of Rpo21p, the largest subunit of RNA-PII (Proudfoot et al., 2002; Proudfoot, 2004; Zhao et al., 1999).

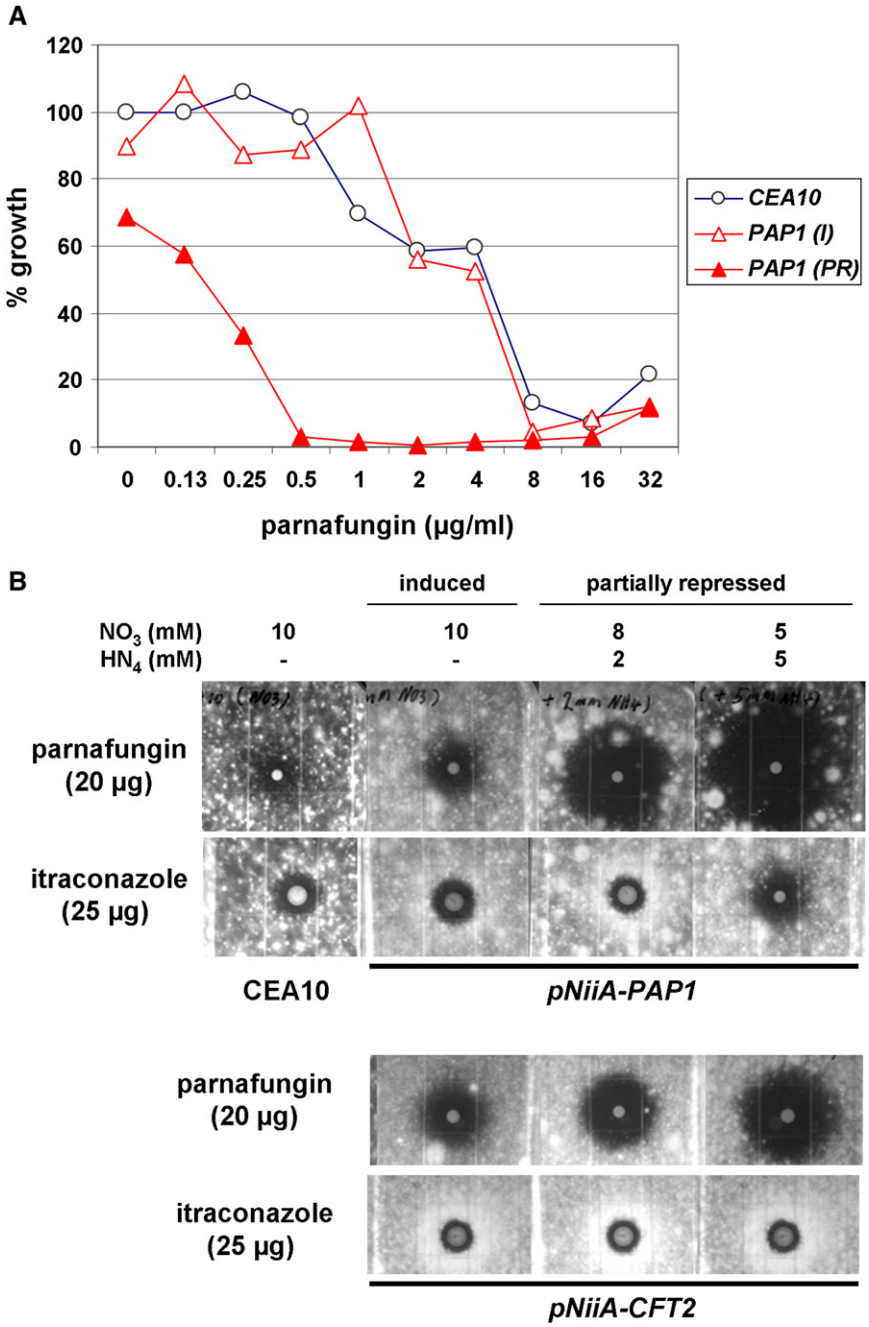

Figure 5. Antifungal Activity of Parnafungin against *A. fumigatus*

(A) Susceptibility of the wild-type strain (CEA10, opened circle) and a pNiiA-Af*PAP1* (*PAP1*) strain, under the inducing conditions (10 mM $Mg(NO_3)_2$, I, opened triangle) and the partially repressing conditions (5 mM $Mg(NO_3)_2$ and 5 mM ammonium tartrate, PR, filled triangle) in AMM liquid medium. The percentage of growth was normalized with that of CEA10 in the absence of parnafungin.

(B) *A. fumigatus PAP1* and *CFT2* conditional mutants are selectively hypersensitive to parnafungin. *pNiiA-AfPAP1* and *pNiiA-AfCFT2* strains were grown under inducing or partially repressing conditions (as indicated by the concentrations of $Mg(NO_3)_2$ (NO_3) and ammonium tartrate (NH_4)) with antifungal compounds added directly on the seeded agar. White spots within the zone of inhibition are due to compound precipitation. Itraconazole is included as a control.

Although *RPO21* was conspicuously absent from parnafungin and cordycepin profiles (despite its inclusion in the strain set), other heterozygotes of subunits of the RNAPII complex (*RPB8*, *RPO26*, and *RPB7*), whose gene products physically interact with the Rpo21p CTD, were resistant to parnafungin. This may reflect a mechanism whereby subtly impairing mRNA transcription in RNAPII heterozygote strains can partially ameliorate compound inhibitory effects on 3′ mRNA processing, thereby restoring a biosynthetic balance between both processes. Although the C/P complex is well characterized in both yeast and metazoans (Proudfoot et al., 2002), the identity of its endonuclease has remained elusive, and only recently has Ysh1p and its human counterpart (CPSF-73) been implicated to confer this function (Ryan et al., 2004). As the *YSH1* heterozygote is the most significantly hypersensitive component of the C/P complex, it may be uniquely supersensitive to parnafungin since both endonuclease and polyadenylation activities would be impaired by heterozygosity and chemical inhibition, respectively. Finally, *POP2* encodes an mRNA deadenylase required for degradation of polyadenylated transcripts in yeast (Daugeron et al., 2001), and a *C. albicans POP2* heterozygote displayed resistance to both parnafungin and cordycepin. Therefore, attenuated mRNA deadenylation by *POP2* heterozygosity may partially remediate the effects of chemical (or genetic) inactivation of PAP.

Chemical-genetic profiles, however, provide only a hypothesis as to the MOA of bioactive natural products, and biochemical and/or genetic confirmation of such predictions are required. To this end, we demonstrate that parnafungin principally effects 3′ mRNA polyadenylation in a yeast cell-free system, and that *C. albicans*, *S. cerevisiae*, and human PAP enzymes are all inhibited by parnafungin, but with *C. albicans* PAP displaying a 4- to 5-fold lower IC_{50} to the compound (Figure 3). We also demonstrate that a F115A substitution in either *C. albicans* PAP allele is sufficient to specifically confer parnafungin resistance (Figure 4; Figure S3). Although, this mutation maps to the ATP-binding domain of PAP, parnafungin does not act as an ATP-competitive inhibitor. Importantly, the in vitro parnafungin IC_{50} values against *C. albicans* PAP strongly correlate with its MIC against this pathogen, reinforcing its primary MOA in whole cells. The lack of a similar correlation between the in vitro and in vivo inhibitory effects of

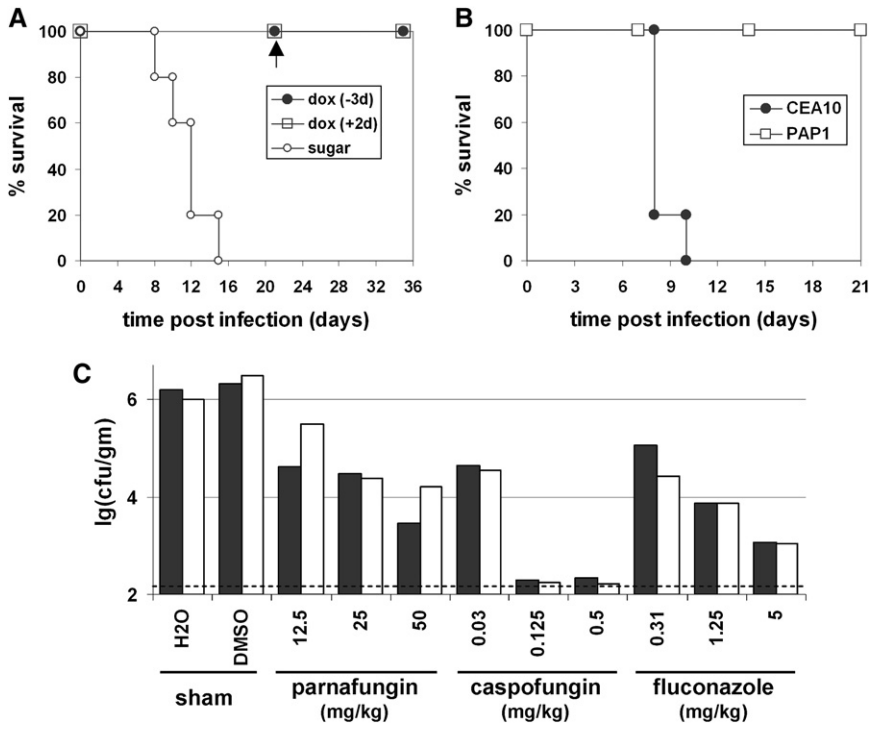

Figure 6. Murine Infection Models Demonstrate PAP Target Essentiality and Parnafungin Efficacy

(A) In vivo target validation of *PAP1* in a murine model of candidiasis. Mice were infected with a *pTET-PAPα/papaΔ* strain and subjected to the following treatments: solid circle, doxycycline given to the mice starting 3 d before infection (Dox-3, prophylactic treatment); open square, doxycycline treatment started 2 d after the infection (Dox+2, symptomatic treatment); open circle, sugar 5% (no doxycycline treatment control). Twenty-one days after infection (indicated by an arrow), all remaining mice stopped receiving doxycycline and were given water instead, until the end of the experiment at day 35 postinfection.

(B) In vivo target validation of *PAP1* in an immunocompromised murine model of aspergillosis. open circle, *pNiiA-PAP1* strain; solid circle, wild-type strain (CEA10), included as a control for virulence.

(C) In vivo efficacy of parnafungin in a systemic model of candidiasis. Mice were treated in two independent experiments (1 and 2, filled and opened bars, respectively) with parnafungin, caspofungin, or fluconazole at the indicated doses (mg/kg). Kidneys were aseptically extracted after treatment, and log reduction in CFU/gm kidney tissue was calculated based on kidney burden of sham treatment. Note that the limit of detection is 1.60×10^2 CFU/gm, as indicated by the dashed line.

parnafungin against *S. cerevisiae* remain unclear, but they may reflect differences in drug uptake, efflux, and/or metabolism. Similarly, differences in parnafungin metabolism by *C. albicans* and mammalian cells may contribute to its efficacy in a murine model of infection, despite potential issues of target-specific toxicity.

Chemical-Genetic Profiling in *C. albicans* and *S. cerevisiae*

Does it matter whether a *C. albicans* or *S. cerevisiae*-based chemical genomics strategy is used? In the case of parnafungin, as its *C. albicans* potency is more than 200-fold greater than *S. cerevisiae* (Table 1), it was beneficial to apply the CaFT, particularly when screening it within a crude extract of low titer. However, other compounds displaying reversed relative potencies, and favoring the use of yeast would be anticipated. It is also true that *NNT1*, which is absent in *S. cerevisiae*, and its heterozygote resistance to cordycepin, but not parnafungin, in CaFT profiles aided in discriminating between the known versus novel compound and prioritizing its isolation. However, *ADO1* and/or RNAPII subunit heterozygote resistance in yeast would similarly capture the distinction between parnafungin and cordycepin profiles. A significant benefit to using a *S. cerevisiae*-based chemical-genetic approach is that full genome coverage is available in the heterozygote collection, thus ensuring that all essential genes are included in analyses, and that the resource is available to the community without restriction.

Chemical-genetic strategies offer powerful probes into the immensity of natural chemical diversity. Genome-scale representation of potential targets against the complexity of components in even one microbial broth produces a multifactorial increase in the effective number of screens performed. Unlike traditional HTS, in which individual "privileged" target(s) are screened against large collections of individual compounds, here potentially hundreds of compounds are screened against thousands of targets in empiric fashion by evaluating a single crude extract. Moreover, a greater understanding of compound MOA can be achieved, reflecting not only its protein target, but genetic and physical interaction networks of the target as well as its metabolism. An important limitation to this approach, however, applies to extracts containing multiple mechanistically distinct bioactive compounds. In such cases, only the most prominent member contributing to the overall growth-inhibitory activity of the extract (either due to its high titer or increased potency) can be reliably assayed; minor but potentially interesting activities would be masked in this way and overlooked. Thus, a breadth of extracts may be screened, but the depth in which they can be evaluated remains limiting without chemical fractionation.

Natural products (beginning with penicillin) have made a significant contribution to antibiotic discovery and provide a logical starting point for identifying new antimicrobial compounds of potential therapeutic utility. However, surprisingly few target-specific and mechanistically characterized natural-product-derived antifungal compounds have been discovered, and even fewer display all of the critical attributes of an antifungal agent, namely, a clear target-based MOA, favorable in vitro potency, spectrum, and efficacy in an animal model of infection (Vicente et al., 2001). The discovery of parnafungin by chemical-genetic screening of natural product suggests that this approach is likely to impact antimicrobial drug discovery and add to the catalog of new bioactive small molecules that act by

target-specific mechanisms across the eukaryote-conserved proteome.

EXPERIMENTAL PROCEDURES

Chemicals, Reagents, and Strains

Reference compounds cerulenin, tunicamycin, brefeldin A, and cordycepin were all purchased from Sigma-Aldrich (St. Louis, USA). Fluconazole (DiFlucan Injection, NDC 0049-3371-26 Lot PS152207) was obtained from Pfizer. Heterozygous deletion and conditional shut-off (Tet-regulatable) stains were described previously (Roemer et al., 2003). They and parnafungin are available for noncommercial use by following the standard Merck Material Transfer Agreement (MTA) and clearance procedures.

C. albicans Fitness Test and Spot Tests

The *C. albicans* fitness test (CaFT) is described by Xu et al. (2007). A summary of heterozygous strains present in the pool is provided in Table S1. Spot tests and liquid assays were performed as described (Xu et al., 2007); specific conditions are provided in legends. Although we are unable to provide the complete heterozygote strain set at this time, we invite academic researchers to contact us regarding possible collaborations related to MOA studies of bioactive compound(s) of mutual interest. Following an MTA executed by both parties, such compounds would be screened by the CaFT, and results would be communicated to the collaborator.

Natural-Product Extracts

Fermentation broths derived from *Sarocladium oryzae* (cerulenin producer), *Eupenicillium brefeldianum* (brefeldin A), *Streptomyces lysosuperficus* (tunicamycin), and *Fusarium larvarum* (MF7022; parnafungin) were grown in liquid medium, extracted with an equal volume of acetone, and filtered. Acetone was removed by blowing with nitrogen, and the aqueous material was examined by CaFT at sub-MICs ranging from IC_{30} to IC_{80}. Isolation of parnafungin is described by C.P., et al. (unpublished data).

Preparation of Whole-Cell Extract, $(NH_4)_2SO_4$ Fractionation, and In Vitro Cleavage and Polyadenylation Assay

The whole-cell extract (WCE) was prepared from *S. cerevisiae* by using the method described by Chen and Moore (1992), with minor modifications that protease inhibitors (1 mM PMSF, 2 μM pepstatin A, and 0.6 μM leupeptin) were added to buffer C. The $(NH_4)_2SO_4$ (40%) precipitate was dissolved in and then dialyzed against buffer D. The final sample was frozen and stored in −80°C until use. The same method was used to prepare WCE from *C. albicans*. The ^{33}P-UTP-labeled RNA substrate was generated by in vitro transcription of linearized plasmid pGAL7-1 by using T3 RNA polymerase as described by Chen and Moore (1992). The standard C/P reaction (20 min at 30°C) was described by the same authors with minor modifications. Each reaction was performed in a total volume of 10 μl, containing 20 mM HEPES (pH 7), 1 mM $Mn(CH_3COO)_2$, 75 mM $K(CH_3COO)$, 2% PEG 8000, 1 mM ATP, 10 mM creatine phosphate, 1 mM DTT, 8 U RNasin, and ~10 ng RNA substrate (~3×10^6 cpm). Extracted RNA product was resolved on a 6% denaturing gel and exposed to a Phosphor Imager screen.

Poly(A) Polymerase Assay

The poly(A) polymerase (PAP) assays were as described by Lingner et al. (1991) with modifications and recombinant *S. cerevisiae* PAP (USB). The reaction (20 min at 30°C) was performed in a 96-well format in a final volume of 20 μl, containing 20 mM Tris (pH 7.0), 50 mM KCl, 0.7 mM $MnCl_2$, 0.2 mM EDTA, 100 μg/ml BSA, 10% glycerol, 40 ng yeast tRNA (Sigma), 6 μM ATP, 0.075 μM ^{3}H-ATP (GE/Amersham), and 50 U PAP, and was stopped by adding 150 μl 10% TCA and 10 mM $Na_4P_2O_7$. The polyadenylated tRNA was captured by GF/C glass filter paper, washed, and countered. A synthetic poly(A) RNA (240 ng/reaction) (Sigma) was used in the native *C. albicans* PAP (from WCE, 0.5%) assay (0.8 μM ATP, 1.5 μM ^{3}H-ATP, 20 mM creatine phosphate, 0.5 mM DTT, 0.1 mg/ml creatine kinase, 40 min at 30°C). In assays with recombinant PAPs (6 μM ATP, 0.075 μM ^{3}H-ATP), 9 ng *C. albicans* PAPα (with 200 ng poly(A), 15 min at 24°C), or 10 ng human PAP (13 ng poly(A), 20 min at 37°C) was used.

Isolation and Characterization of Parnafungin-Resistant Mutants

EMS mutagenesis was performed according to Guthrie and Fink (1991). Cultures of the *PAPα/papaΔ* (CA35) and the *HIS3/his3Δ* (CA12) strains were treated with EMS at a survival rate of ~10%. The surviving cells were plated directly on YNBD agar containing 100 ng/ml parnafungin. A total of 3×10^7 and 1×10^7 surviving cells from CA35 and CA12 strains, respectively, were screened. After two rounds of selection, the resistant isolates were tested for resistance to fluconazole (at 2 and 4 μg/ml) and aureobasidin A (at 20, 30, and 40 ng/ml). The entire coding sequences of *PAPα* from selected mutants were PCR amplified, cloned, and fully sequenced. A two-step gene replacement strategy (Guthrie and Fink, 1991) was used to introduce a *papα(F115I)* chromosomal mutation in CA35 (see Figure S3A for details). The pop-in transformants (e.g., CA153, containing tandem repeats of *papα(F115I)::URA3::PAPα*) were selected, and correct integration was confirmed by PCR. They were subsequently selected for the loss of *papα* or *PAPα*. The corresponding ORFs from the resulting pop-out strains were PCR amplified, cloned, and sequenced. Those containing *papα(F115I)* (e.g., CA164, derived from CA153) or *PAPα*, together with the parental pop-in strains, were tested for susceptibility to parnafungin (Figure S3B). The *papa(F115I)* mutation was constructed by site-directed mutagenesis (QuickChange, Stratagene). It was introduced into the *PAPa/papαΔ* strain (CA226) in a similar manner.

C. albicans and *A. fumigatus* Virulence Studies

The murine model of systemic candidiasis was described by Roemer et al. (2003). Three groups of ICR mice were each infected by tail-vein injection (10^6 cells of the *pTET-PAPα/papaΔ* strain) and were examined: (1) Dox-3, receiving the doxycycline treatment 3 d (in the drinking water, at 2 mg/ml and 5% sucrose) prior to infection; (2) Dox +2, receiving the doxycycline treatment 2 d after infection; and (3) the control, receiving only 5% sucrose for the duration of the experiment. After 21 d postinfection, two mice from each group were taken for necropsy, and the remaining mice were switched to water. The survival of these mice was monitored for an additional 2 weeks, and additional necropsies were performed thereafter. The virulence of the *pNiiA-PAP1 A. fumigatus* mutant was assessed in a murine model for systemic aspergillosis as described previously (Hu et al., 2007). All experiments were performed according to the National Institutes of Health guidelines for the ethical treatment of animals.

In Vivo Efficacy Evaluation of Parnafungin

To evaluate parnafungin in vivo activity, a previously described model of disseminated candidiasis with hypersusceptibility to *C. albicans* and increased sensitivity for discriminating antifungal efficacy was used (Bartizal et al., 1992). Immunosuppressed DBA/2N mice were challenged intravenously with either 7.6×10^4 (experiment 1) or 3.0×10^4 (experiment 2) *C. albicans* MY1055 and treated with 50, 25, or 12.5 mg/kg parnafungin (4 mice/group) administered intraperitoneally twice daily over 2 d (4 doses). Fluconazole and caspofungin were used as controls, and 10% DMSO was used as a sham. After 48 hr, the mice were sacrificed, and burden of infection was determined by cfu per gram of homogenized kidney.

SUPPLEMENTAL DATA

Supplemental Data include five figures, three tables, and a spreadsheet containing the complete *C. albicans* heterozygote strain set as well as their z-scores in all Fitness Test experiments described in the manuscript and are available at http://www.chembiol.com/cgi/content/full/15/4/363/DC1/.

ACKNOWLEDGMENTS

We thank Mary Ann Powles, Drew Misura, Lynn Gercken, Emily Hickey, Mary Motyl, Li-Yin Huang, Kara Stillmock, and Deborah Zink for technical support and Claire Moore and Xiaoyuan He for reagents and advice regarding the cleavage and polyadenylation assay. We also thank Howard Bussey for his critical reading of the manuscript and Pam Ocampo for her operational excellence in managing the Center of Fungal Genetics. This work was supported in part by Genome Canada and Genome Quebec. Some of the authors are employees of Merck & Co., Inc., as stated in the affiliations, and potentially own stock and/or hold stock options in the Company.

Received: December 18, 2007
Revised: February 21, 2008
Accepted: February 22, 2008
Published: April 18, 2008

REFERENCES

Baetz, K., McHardy, L., Gable, K., Tarling, T., Reberioux, D., Bryan, J., Andersen, R.J., Dunn, T., Hieter, P., and Roberge, M. (2004). Yeast genome-wide drug-induced haploinsufficiency screen to determine drug mode of action. Proc. Natl. Acad. Sci. USA *101*, 4525–4530.

Bartizal, K., Abruzzo, G., Trainor, C., Krupa, D., Nollstadt, K., Schmatz, D., Schwartz, R., Hammond, M., Balkovec, J., and Vanmiddlesworth, F. (1992). In vitro antifungal activities and in vivo efficacies of 1,3-β-D-glucan synthesis inhibitors L-671,329, L-646,991, tetrahydroechinocandin B, and L-687,781, a papulacandin. Antimicrob. Agents Chemother. *36*, 1648–1657.

Chen, J., and Moore, C. (1992). Separation of factors required for cleavage and polyadenylation of yeast pre-mRNA. Mol. Cell. Biol. *12*, 3470–3481.

Clardy, J., Fischbach, M.A., and Walsh, C.T. (2006). New antibiotics from bacterial natural products. Nat. Biotechnol. *24*, 1541–1550.

Daugeron, M.C., Mauxion, F., and Séraphin, B. (2001). The yeast POP2 gene encodes a nuclease involved in mRNA deadenylation. Nucleic Acids Res. *29*, 2448–2455.

Giaever, G., Shoemaker, D.D., Jones, T.W., Liang, H., Winzeler, E.A., Astromoff, A., and Davis, R.W. (1999). Genomic profiling of drug sensitivities via induced haploinsufficiency. Nat. Genet. *21*, 278–283.

Giaever, G., Chu, A.M., Ni, L., Connelly, C., Riles, L., Veronneau, S., Dow, S., Lucau-Danila, A., Anderson, K., Andre, B., et al. (2002). Functional profiling of the *Saccharomyces cerevisiae* genome. Nature *418*, 387–391.

Giaever, G., Flaherty, P., Kumm, J., Proctor, M., Nislow, C., Jaramillo, D.F., Chu, A.M., Jordan, M.I., Arkin, A.P., and Davis, R.W. (2004). Chemogenomic profiling: identifying the functional interactions of small molecules in yeast. Proc. Natl. Acad. Sci. USA *101*, 793–798.

Guthrie, C., and Fink, G.R., eds. (1991). Guide to Yeast Genetics and Molecular Biology (Methods in Enzymolology) (New York: Academic Press).

Hu, W., Sillaots, S., Lemieux, S., Davison, J., Kauffman, S., Breton, A., Linteau, A., Xin, C., Bowman, J., Becker, J., et al. (2007). Essential gene identification and drug target prioritization in *Aspergillus fumigatus*. PLoS Pathog. *3*, e24.

Hughes, T.R., Marton, M.J., Jones, A.R., Roberts, C.J., Stoughton, R., Armour, C.D., Bennett, H.A., Coffey, E., Dai, H., He, Y.D., et al. (2000). Functional discovery via a compendium of expression profiles. Cell *102*, 109–126.

Hull, C.M., and Johnson, A.D. (1999). Identification of a mating type-like locus in the asexual pathogenic yeast *Candida albicans*. Science *285*, 1271–1275.

Kerwitz, Y., Kühn, U., Lilie, H., Knoth, A., Scheuermann, T., Friedrich, H., Schwarz, E., and Wahle, E. (2003). Stimulation of poly(A) polymerase through a direct interaction with the nuclear poly(A) binding protein allosterically regulated by RNA. EMBO J. *15*, 3705–3714.

Koehn, F.E., and Carter, G.T. (2005). The evolving role of natural products in drug discovery. Nat. Rev. Drug Discov. *4*, 206–220.

Lecoq, K., Belloc, I., Desgranges, C., and Daignan-Fornier, B. (2001). Role of adenosine kinase in *Saccharomyces cerevisiae*: identification of the ADO1 gene and study of the mutant phenotypes. Yeast *18*, 335–342.

Lingner, J., Radtke, I., Wahle, E., and Keller, W. (1991). Purification and characterization of poly(A) polymerase from *Saccharomyces cerevisiae*. J. Biol. Chem. *266*, 8741–8746.

Loewen, S.K., Ng, A.M., Mohabir, N.N., Baldwin, S.A., Cass, C.E., and Young, J.D. (2003). Functional characterization of a H^+/nucleoside co-transporter (CaCNT) from *Candida albicans*, a fungal member of the concentrative nucleoside transporter (CNT) family of membrane proteins. Yeast *20*, 661–675.

Lum, P.Y., Armour, C.D., Stepaniants, S.B., Cavet, G., Wolf, M.K., Butler, J.S., Hinshaw, J.C., Garnier, P., Prestwich, G.D., Leonardson, A., et al. (2004). Discovering modes of action for therapeutic compounds using a genome-wide screen of yeast heterozygotes. Cell *116*, 121–137.

Muller, W.E., Seibert, G., Beyer, R., Breter, H.J., Maidhof, A., and Zahn, R.K. (1977). Effect of cordycepin on nucleic acid metabolism in L5178Y cells and on nucleic acid-synthesizing enzyme systems. Cancer Res. *37*, 3824–3833.

Newman, D.J., Cragg, G.M., and Snader, K.M. (2003). Natural products as sources of new drugs over the period 1981–2002. J. Nat. Prod. *66*, 1022–1037.

Park, S., Kelly, R., Kahn, J.N., Robles, J., Hsu, M.J., Register, E., Li, W., Vyas, V., Fan, H., Abruzzo, G., et al. (2005). Specific substitutions in the echinocandin target Fks1p account for reduced susceptibility of rare laboratory and clinical *Candida sp*. isolates. Antimicrob. Agents Chemother. *49*, 3264–3273.

Parsons, A.B., Lopez, A., Givoni, I.E., Williams, D.E., Gray, C.A., Porter, J., Chua, G., Sopko, R., Brost, R.L., Ho, C.H., et al. (2006). Exploring the mode-of-action of bioactive compounds by chemical-genetic profiling in yeast. Cell *126*, 611–625.

Payne, D.J., Gwynn, M.N., Holmes, D.J., and Pompliano, D.L. (2007). Drugs for bad bugs: confronting the challenges of antibacterial discovery. Nat. Rev. Drug Discov. *6*, 29–40.

Petrikkos, G., and Skiada, A. (2007). Recent advances in antifungal chemotherapy. Int. J. Antimicrob. Agents *30*, 108–117.

Proudfoot, N.J. (2004). New perspectives on connecting messenger RNA 3′ end formation to transcription. Curr. Opin. Cell Biol. *16*, 272–278.

Proudfoot, N.J., Furger, A., and Dye, M.J. (2002). Integrating mRNA processing with transcription. Cell *108*, 501–512.

Reddy, C.S., and Reddy, S.V. (1991). Secalonic acids. In Mycotoxins and Phytoalexins, R.P. Sharma and D.K. Salunkhe, eds. (Florida: CRC Press, Inc.), pp. 167–190.

Rodriguez-Suarez, R., Xu, D., Veillette, K., Davison, J., Sillaots, S., Kauffman, S., Hu, W., Bowman, J., Martel, N., Trosok, S., et al. (2007). Mechanism-of-action determination of GMP synthase inhibitors and target validation in *Candida albicans* and *Aspergillus fumigatus*. Chem. Biol. *14*, 1163–1175.

Roemer, T., Jiang, B., Davison, J., Ketela, T., Veillette, K., Breton, A., Tandia, F., Linteau, A., Sillaots, S., Marta, C., et al. (2003). Large-scale essential gene identification in *Candida albicans* and applications to antifungal drug discovery. Mol. Microbiol. *50*, 167–181.

Ryan, K., Calvo, O., and Manley, J.L. (2004). Evidence that polyadenylation factor CPSF-73 is the mRNA 3′ processing endonuclease. RNA *10*, 565–573.

Safdar, A., Chaturvedi, V., Cross, E.W., Park, S., Bernard, E.M., Armstrong, D., and Perlin, D.S. (2001). Prospective study of *Candida* species in patients at a comprehensive cancer center. Antimicrob. Agents Chemother. *45*, 2129–2133.

Shoemaker, D.D., Lashkari, D.A., Morris, D., Mittmann, M., and Davis, R.W. (1996). Quantitative phenotypic analysis of yeast deletion mutants using a highly parallel molecular bar-coding strategy. Nat. Genet. *14*, 450–456.

Vicente, M.F., Cabello, A., Platas, G., Basilio, A., Diez, M.T., Dreikorn, S., Giacobbe, R.A., Onishi, J.C., Meinz, M., Kurtz, M.B., et al. (2001). Antimicrobial activity of ergokonin A from *Trichoderma longibrachiatum*. J. Appl. Microbiol. *91*, 806–813.

Winzeler, E.A., Shoemaker, D.D., Astromoff, A., Liang, H., Anderson, K., Andre, B., Bangham, R., Benito, R., Boeke, J.D., Bussey, H., et al. (1999). Functional characterization of the *S. cerevisiae* genome by gene deletion and parallel analysis. Science *285*, 901–906.

Xu, D., Jiang, B., Ketela, T., Lemieux, S., Veillette, K., Martel, N., Davison, J., Sillaots, S., Trosok, S., Bachewich, C., et al. (2007). Genome-wide Fitness Test and mechanism-of-action studies of inhibitory compounds in *Candida albicans*. PLoS Pathog. *3*, e92.

Yim, G., Huimi, H., and Davies, J. (2006). The truth about antibiotics. Int. J. Med. Microbiol. *296*, 163–170.

Zhao, J., Hyman, L., and Moore, C. (1999). Formation of mRNA 3′ ends in eukaryotes: mechanism, regulation, and interrelationships with other steps in mRNA synthesis. Microbiol. Mol. Biol. Rev. *63*, 405–445.

